Alignment of the 2P state of 2-MeV/amu heliumlike sulfur

D. A. Church, R. A. Kenefick, D.-W. Wang,* and R. L. Watson
Department of Physics and Cyclotron Institute, Texas A&M University, College Station, Texas 77843
(Received 28 June 1982)

The 2^1P and 2^3P levels of two-electron S XV have been aligned by collision at 2 MeV/amu with carbon atoms in a foil. The degree of alignment is obtained by analysis of the normalized angular distribution of K x-ray radiation measured in high resolution with a pivoted plane-crystal Bragg spectrometer. The mean cross-section ratio σ_0/σ_1 for population of the $m=0$ sublevel relative to the $m=\pm1$ sublevels of the $2P$ parent state is obtained by analysis of the 1^1S-2^1P and 1^1S-2^3P transition intensities. The result $\sigma_0/\sigma_1=1.79\pm0.1$ leads to the polarization fractions $P(^1P)=0.28\pm0.05$, and $P(^3P)=-0.16\pm0.03$, in good agreement with results obtained by an independent analysis, and in excellent agreement with coupled-states calculations of Reading *et al.* Comparison with other theories is also made.

I. INTRODUCTION

The linear polarization of radiation emitted in electromagnetic transitions is determined by the relative populations of the magnetic sublevels of the excited atomic states. These populations are related to the cross sections for production of the sublevels produced in the exciting collision. This information enables a more stringent test of theory of the excitation process than does a measurement of a total cross section, which averages over the states created with preferred directions of angular momentum. The production of collisional anisotropy in fast ions makes possible spectroscopic measurements of atomic and nuclear parameters,[1] such as coherence measurements of atomic and nuclear g factors.[2–4]

In the course of a recent high-resolution investigation of the K x-ray spectrum of highly stripped sulfur ions,[5] it was noted that the relative intensities of the x-ray transitions originating from the 2^1P and 2^3P levels of heliumlike sulfur varied with the spectrometer observation angle. As it is often advantageous to use spectrometer angles other than 90° for improved resolution,[5] or for Doppler tuned spectrometric purposes,[6] an understanding of any underlying physical process which may affect the angular distribution of radiation from different levels is important. Anisotropy in excitation may also have effects on the determination of mean lives of excited levels, either directly or following a cascade process.[7]

Other experimental studies have shown that the relative intensities of the 1^1S-2^1P and 1^1S-2^3P transitions vary with the exciting foil surface density,[8] due to the relatively long mean life of the 2^3P level compared to the prompt transition from the 2^1P level. Any ^3P levels produced inside the foil tend to be quenched by subsequent collisions before radiating, while the prompt ^1P radiation is collected from both inside and outside the target foil with only modest collision broadening. Thus the ^3P radiation intensity and polarization are potentially sensitive to effects associated with near-surface excitation, while the ^1P intensity and polarization reflect the bulk excitation process. A difference between surface and bulk excitation processes was observed in the measurements of Hass *et al.*[3] and Goldring *et al.*,[4] where nuclear orientation by coupling to inclined-foil atomic orientation produced a perturbed angular correlation. No orientation of atomic levels by bulk excitation has yet been observed or predicted theoretically.[9] At significantly lower energies than discussed here, differences between 3^3P and 3^1P anisotropic excitation of neutral helium by foil collision have been measured.[10] However, in the inner-shell excitation reported here, the atomic character of the collision is expected to dominate the bulk or surface effects.

Some recent theoretical support has been given to the possibility that the orientation and alignment of excited levels in collisions of ions with inclined targets arises from interaction with localized target states (e.g., atoms).[11] Inner-shell ionization or capture processes almost certainly occur through individual ion-atom interactions, since the velocity matching of the active electron to the projectile requires velocities characteristic of inner-shell electrons. Consequently, the comparison of interactions which produce or fill K or L vacancies with interaction occurring at lower collision energies which

match outer-shell electron velocities may be useful in defining the atomic character of the total ion-target interaction.

A new addition to the theoretical approximation methods used to analyze high-velocity ion-atom collisions is the "one and a half centered" (OHCE) atomic-orbital expansion method of Reading, Ford, and Becker.[12–14] The OHCE retains the calculational speed of the coupled-channels single center expansion method, but improves on it by taking account of the loss of flux into electron-capture channels. This method has been used to compute total summed-over-m cross sections for excitation, ionization, and capture; examples of applications to specific collision systems and comparison to experiment are given in the above references. The OHCE method also predicts absolute cross sections for excitation or capture to individual magnetic sublevels of excited states.[15] This aspect has not been previously tested, owing to the lack of data. The method has now been used to calculate capture at 2 MeV/amu from the $1s$ level of carbon into the $2p$ level of sulfur. Since capture is expected to be the predominant process for the production of the heliumlike $2p$ states studied in the present measurements, comparison of the predictions of this calculation with the experimental results, discussed below, provides additional support for the utility of the OHCE theory.

II. BACKGROUND OF THE METHOD

The polarization fraction for linearly polarized light is defined as

$$P=(I_{||}-I_{\perp})/(I_{||}+I_{\perp})$$

in terms of the intensities of radiation emitted at 90° to the exciting ion beam direction, polarized, respectively, parallel ($I_{||}$) and perpendicular ($I_{\perp}$) to this beam direction. The polarization fraction is a measure of the anisotropy introduced into the excited sublevel populations by the excitation process; it can therefore be related to the cross sections for excitation of these sublevels. Since direct coupling to the electron spin during the collision is expected to be negligible, the cross sections apply to the orbital quantum numbers only. The subsequent coupling of the electron spin to the orbital motion via the spin-orbit interaction reduces the polarization fraction from the value it would assume in the absence of such coupling.[16] Further coupling to the nuclear spin is possible,[17] but is expected to be negligible for the short-lived P states of interest here. Percival and Seaton[16] have shown that

$$P(^1P)=(\sigma_0-\sigma_1)/(\sigma_0+\sigma_1)$$

and

$$P(^3P)=-(\sigma_0-\sigma_1)/(\sigma_0+3\sigma_1)$$

for the $2p$-$1s$ transitions in heliumlike ions, where σ_0 and σ_1 are the cross sections for populating the $m=0$ and $m=\pm 1$ substates, respectively.

Jamison *et al.*[18–20] have measured the polarization fraction of K x-rays directly by using the polarizing properties of a Bragg crystal. When the Bragg angle is equal to the Brewster angle of the crystal, a rotation of the spectrometer about the incident photon axis (at 90° to the ion beam direction) provides a direct measure of the polarization fraction P. When the Bragg angle departs from the Brewster angle, as it must for most transitions, corrections dependent on the (generally unknown) crystal reflectivity are required.[21,22] Since the spectra containing the sulfur K x-rays of interest here are recorded with a NaCl crystal at a range of Bragg angles far from the Brewster angle, an angular distribution measurement was attempted. In principle, this yields the same polarization information. Low (energy) resolution angular distribution measurements of certain target and beam K x-ray transitions have beem made previously by Ellsworth *et al.*[23,24] using Si(Li) detectors.

The angular distribution of radiation in the reference frame of the emitters is expressed in terms of the polarization fraction, and of the angle θ between the forward (downstream) beam direction and the axis for light collection by

$$I(\theta)=I_{90}(1-P\cos^2\theta)\ ,$$

where I_{90} is the intensity measured at 90°. This angular dependence can also be expressed in terms of the Fano-Macek orientation and alignment parameters.[17] Radiation from a projectile moving at $v/c=0.06$ (2 MeV/amu) requires additional relativistic corrections. The reflectivity of a Bragg crystal spectrometer varies strongly with both the Bragg angle and the polarization of the incident radiation. Calibration of these dependences using the transitions investigated here are described by Wang *et al.*,[25] hereafter denoted Ref. A. An alternative to the procedure used in Ref. A is to normalize the angular distribution of a polarized transition to that of an unpolarized transition in the same spectrum. This provides a direct measure of the relative angular distribution. If a transition for which polarization is forbidden by the symmetry of the system is

not present in the spectrum, relative polarization fractions can still be obtained and subsequently normalized to an absolute polarization calibration. This is the procedure that has been adopted here, since partial polarization of the various other x-ray lines lying near the transitions of interest is likely.

The angular distribution of the ratio of the intensities of the 1^1S-2^1P and 1^1S-2^3P transitions is a function of the polarization fractions $P(^1P)$ and $P(^3P)$ and the angle θ. The advantage of using an angular distribution ratio is that the ratio is relatively insensitive to the effects of crystal reflectivity and absorption. One might fit the data to this function to simultaneously obtain the two polarization fractions. A superior choice is to use the relationships of the polarization fractions to the cross sections σ_0 and σ_1 to construct a theoretical expression for the transition intensity ratio which is a function only of σ_0/σ_1, the intensity ratios at 90°, and θ. The cross-section ratio σ_0/σ_1 is obtained from the fit, and from this result the polarization fractions may be calculated and compared to the results obtained in direct determinations from fits to the angular distributions of the intensities.

III. EXPERIMENTAL METHODS

The collision and detection geometry, and the rotatable, plane-crystal Bragg spectrometer are diagrammed in Fig. 1. A beam of charge-to-momentum selected 2-MeV/amu (+ 5) sulfur ions accelerated by the Texas A&M Variable Energy Cyclotron was focused using a fluorescent target, and

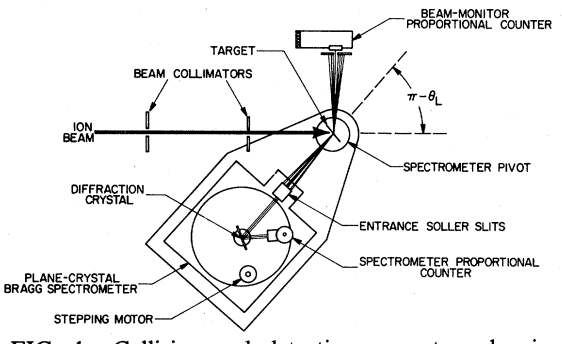

FIG. 1. Collision and detection geometry, showing the relationship of target carbon foil to rotatable Bragg plane-crystal spectrometer and monitor counter. Foil was rotated 90° when downstream angles were observed, but remained at 45° to beam axis. Spectrometer angle θ_L was defined relative to downstream beam direction. Geometric limitations restricted θ_L to the range of $20° \leq \theta \leq 161°$.

subsequently directed onto a nominal 80 $\mu g/cm^2$ carbon foil inclined at an angle of 45° to the beam direction about an axis perpendicular to the plane containing the beam and spectrometer. This angle was set at either $+45°$ or $-45°$ for forward or backward spectrometer observation angles, respectively, so that the spectrometer viewed a broad surface of the foil. The angles were set using a digital angle calibrator, and spectra were checked for possible angle-related errors; none were observed. The spectrometer was pivoted in a horizontal plane about an axis coincident with the foil rotation axis. The spectrometer observation angles ranged from 20° to $\simeq$160° with respect to the heavy-ion beam direction. At the largest angle, the beam passed through an open portion of the spectrometer itself. X-rays emitted from the sulfur ions were collimated with Soller slits having a plate spacing of 0.013 cm, and were diffracted by a plane NaCl crystal. The diffracted x rays passed through another Soller slit collimater having twice the plate spacing of the entrance slits (primarily for background rejection) into a gas-flow proportional counter (90% argon and 10% methane at 1 atm) equipped with a 530-$\mu g/cm^2$ Mylar window.

Several beam normalization systems were tested, including integration of the beam current generated in the target foil, and measurement of Rutherford scattered ions from an upstream foil using a solid-state detector. The final, and most satisfactory, method involved the use of a second proportional counter having specifications identical to the one described above, mounted with a direct view of the sulfur x-rays produced at the target foil.

The spectrometer counter and monitor counter signals were processed by two identical electronic systems, each consisting of a preamplifier, a spectroscopy amplifier, and a single-channel analyzer for pulse height discrimination. The x-ray signals from the monitor system were scaled by a spectrometer controller which automatically advanced the Bragg angle by 0.046° each time the preset monitor count was reached. The preset monitor count was set sufficiently high to make statistical fluctuations associated with the measurement of the diffracted x-ray intensity negligible compared to other uncertainties. The diffracted x-ray intensity measured at each Bragg angle was sent to a VAX 11/780 computer system via a CAMAC interface, where plotting and analysis procedures were performed upon completion of the spectral scan. Spectra obtained at the observation angles 140° and 55° are compared in Fig. 2. Differences in the relative

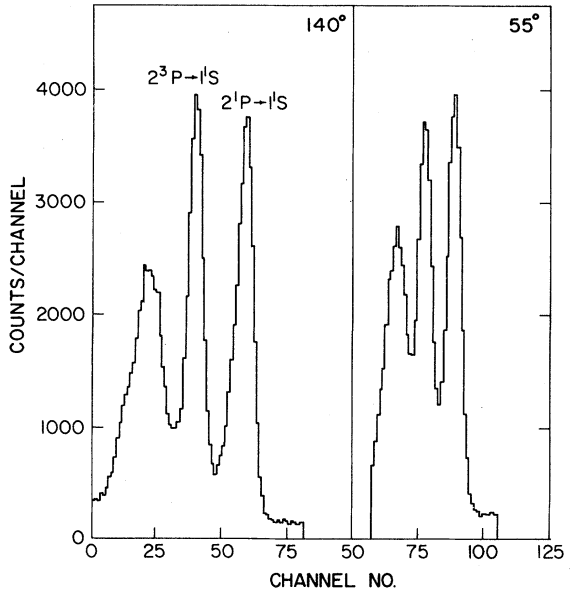

FIG. 2. Spectra of heliumlike sulfur K x-rays taken at angles of 55° and 140°. Note compression of 55° spectrum due to Doppler effect on x-ray energies. Relative intensities of transitions from ^1P and ^3P levels change significantly as a function of observation angle.

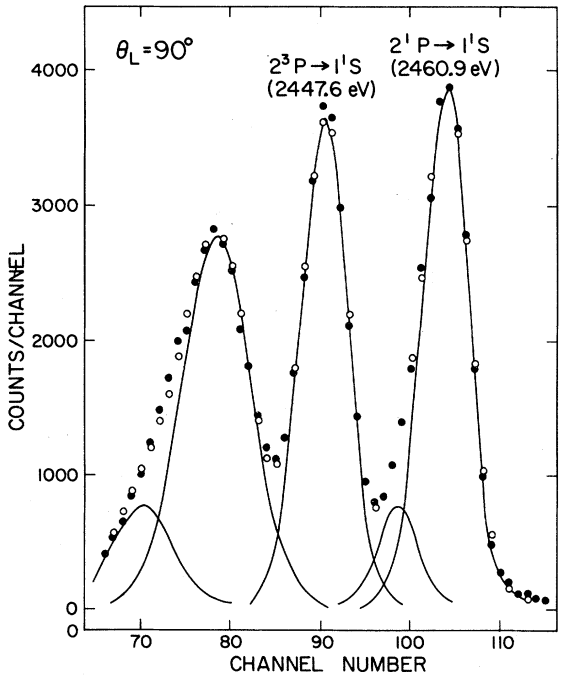

FIG. 3. Example of a fitted sulfur K x-ray spectrum, emphasizing heliumlike transitions taken at a spectrometer angle of 90°. Filled circles represent data points, and open circles represent calculated points. Spectral feature lying between heliumlike transitions is thought to arise either from shifted ^1S-^1P x-rays emitted from within foil, or to a spectator line (Li-like transition).[5]

intensities of the ^1P and ^3P peaks are clearly visible in these spectra. Also, the 55° spectrum is considerably compressed relative to the 140° spectrum as a consequence of the Doppler effect.

The spectra were analyzed by means of a least-square-fitting program (FACELIFT). The small background in each spectrum was represented by a straight line with variable slope and intercept, and the component x-ray lines were represented by Voigt functions. The ^1P transition was found to require a Lorentzian component due to collision broadening inside the foil, but the Lorentzian width of the ^3P transition was set to zero. An example of a fitted spectrum of sulfur projectile x-rays is shown in Fig. 3. The areas under the peaks are proportional to the emitted x-ray intensities normalized to the incident beam flux by the monitor count. A spectral feature lying between the ^1P and ^3P peaks was identified previously,[26] and is interpreted as being a combination of shifted ^1P x rays emitted inside the foil and x rays from a Li-like spectator-electron configuration. It was possible to fit this spectral feature rather well, but nevertheless, its presence introduced uncertainties in the fitted intensities of the ^1P and ^3P transitions which are larger than those expected on the basis of counting statistics alone. This problem becomes particularly pronounced at the forward angles, where the spectrum is compressed by the Doppler effect.

IV. RESULTS AND DISCUSSION

In order to check the feasibility and reliability of angular distribution measurements performed with the crystal spectrometer system, a preliminary study of the angular distribution of Al K x rays excited by 32-MeV oxygen ions incident on an aluminum target was carried out. A PET (pentaerythritol) diffraction crystal was used to obtain the spectra. In this case, where x rays from stationary target atoms are involved, the Bragg angle is independent of the spectrometer observation angle. A fitted portion of the Al spectrum containing the KL^0, KL^1, and KL^2 multiplet groups is shown in Fig. 4. The KL^0 peak, consisting of the $K\alpha_{1,2}$ transition pair, is expected to be unpolarized, since the initial state is an S state. The KL^2 peak is composed of 14 different multiplet transitions, and hence one may expect it to have only a small polarization at most. Based on the earlier work of Jamison *et al.*[18–20] using 1–3-MeV/amu He, Li, and O ions, the KL^1 peak is ex-

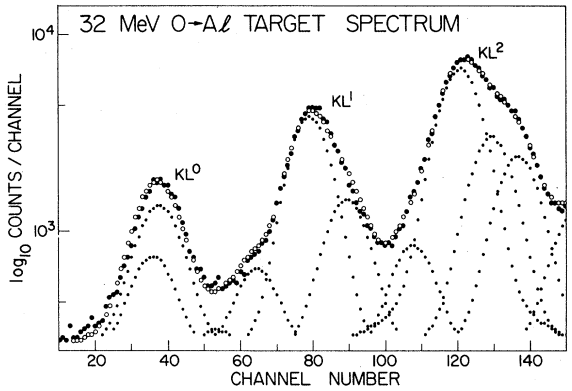

FIG. 4. Spectrum of aluminum target K x-rays showing KL^0, KL^1, and KL^2 multiplets fit with analysis program. KL^0 multiplet is composed of the $K\alpha_{1,2}{}^2S$-^2P transitions.

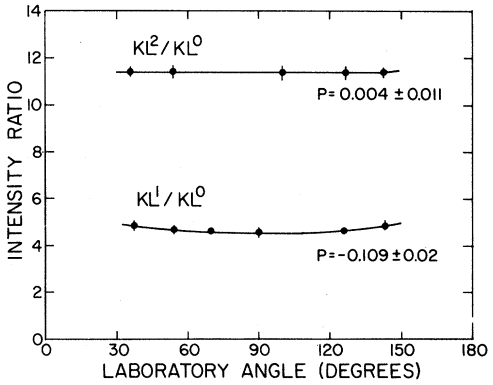

FIG. 5. Angular distribution of aluminum target KL^1 and KL^2 x-ray intensities measured relative to unpolarized $K\alpha_{1,2}$ transitions. The KL^2 group contains a number of transitions, and is expected to have no net polarization, while the KL^1 group is expected to have a net negative polarization fraction, as is verified by observed angular distribution.

pected to have a net negative polarization fraction.

Shown in Fig. 5 (top) are the Al KL^2/KL^0 intensity ratios obtained in the present work. One sees that these ratios are independent of angle, having a fitted value of the polarization fraction

$$P(KL^2)=0.004\pm0.011 .$$

This result shows that the spectrometer system has no significant intrinsic dependence on observation angle. The KL^1 peak consists of five multiplet transitions, of which the most intense are the $K\alpha_3(^3P$-^3P and ^3S-$^3P)$ and the $K\alpha_4(^1P$-$^1D)$. The most strongly polarized component of the KL^1 peak was found by Jamison *et al.*[18–20] to be the $K\alpha'$ transition. Unfortunately, the energy resolution in the present measurements was not sufficient to enable a meaningful analysis of this very weak component. However, the initial-state P levels of the $K\alpha_3$ and $K\alpha_4$ transitions can also be collisionally aligned. In these two cases, the polarization fractions and the sublevel cross sections are related by the formulas[18]

$$P(K\alpha_3)=-15(\sigma_0-\sigma_1)/(67\sigma_0-149\sigma_1) ,$$

$$P(K\sigma_4)=(\sigma_0-\sigma_1)/(7\sigma_0+13\sigma_1) .$$

Full spin-orbit coupling is assumed for the P state. In general $|\sigma_0| > |\sigma_1|$, and so it is to be expected that $P(K\alpha_3)$ will be negative, giving the entire KL^1 peak a negative polarization fraction due to the high relative intensity of the $K\alpha_3$ components (see Fig. 4). This was indeed found to be the case, as may be seen in Fig. 5 (bottom) where the best fit to the intensity ratio of KL^1/KL^0, given a value

$$P=-0.109\pm0.02 ,$$

is shown. The sign of the above result is in agreement with the earlier measurements of Jamison *et al.*; however, the magnitude is significantly larger.

The analysis of transition intensities from fast-moving projectile ions is complicated by the Doppler effect, which (as noted above) causes a dependence of the Bragg angle on the observation angle, thereby requiring a calibration of the crystal reflectivity for absolute intensity comparisons at different observation angles. Such a calibration was carried out, as reported in Ref. A, for the case of He-like S ion x rays analyzed by a NaCl crystal. It was determined in this study that the best representation of the data was given by a reflectivity function described as "perfect crystal with absorption."[25,27] The best least-squares fits to the data with the polarization fraction P set as an adjustable parameter, yielded

$$P(^1P)=0.35\pm0.05$$

and

$$P(^3P)=-0.11\pm0.05 .$$

However, other reflectivity functions with different assumed polarization fractions could also be fit reasonably well to the data. In the work reported here, the angular distribution of relative intensities of the ^1P and ^3P transitions are analyzed.

If in the emitter rest frame

$$N_1(\theta)=N_1^0(1-P_1\cos^2\theta)$$

and

$$N_2(\theta)=N_2^0(1-P\cos^2\theta)$$

then the ratio is

$$N_1(\theta)/N_2(\theta)=(N_1^0/N_2^0)(1-P_1\cos^2\theta)\times(1-P_2\cos^2\theta)^{-1}\,, \qquad (1)$$

where $N_1(\theta)$ and $N_2(\theta)$ are the ^3P and ^1P intensities, respectively, recorded in the angular distribution measurement at each angle θ. When the transition intensities are transformed to the laboratory frame and dispersed by a spectrometer, the expressions are complicated by the crystal reflectivity dependence of the Bragg angle and the Lorentz transformation of angles and energies, as discussed in Ref. A.

The expression for the measured x-ray intensity obtained with a perfect crystal with absorption, as a function of laboratory angle θ_L, is (Ref. A)

$$N(\theta_L)=\frac{\epsilon(\lambda)AN_{90}}{\mu(E)(1-\beta\cos\theta_L)^2}\left[\left[\frac{1-P}{4}\right]\tan\theta_\beta(1-|\cos2\theta_\beta|)+\frac{\sin^2\theta_\beta}{\sin2\theta_\beta}|\cos2\theta_\beta|\times\{1-P[(\cos\theta_L-\beta)/(1-\beta\cos\theta_L)]^2\}\right].$$

Here θ_β is the spectrometer Bragg angle (which depends upon θ_L), N_{90} is the x-ray count at $\theta_L=90°$, and A is composed of constants or slowly varying functions. $\epsilon(\lambda)$ and $\mu(E)$ are the detector efficiency and crystal absorption coefficient, respectively. For the closely spaced transitions originating from the ^1P and ^3P states, $\epsilon(\lambda)\simeq\epsilon(\lambda')$, $\mu(E)\simeq\mu(E')$, and $\theta_\beta\simeq\theta'_\beta$, where the primed quantities denote parameters associated with the ^3P transition. The ratio of x-ray counts for the two transitions can then be written

$$\frac{N(^3P,\theta'_L)}{N(^1P,\theta_L)}=\frac{N'_{90}(1+|\cos2\theta'_\beta|(2-\cos^2\theta)+(\sigma_0/\sigma_1)(1+|\cos2\theta'_\beta|\cos^2\theta)}{N_{90}(1+|\cos2\theta_\beta|\cos^2\theta)+(\sigma_0/\sigma_1)|\cos2\theta_\beta|(1-\cos^2\theta)}\times(\sigma_0/\sigma_1+1)/(\sigma_0/\sigma_1+3)\,,$$

where

$$\cos\theta=(\cos\theta_L-\beta)/(1-\beta\cos\theta_L)\,,$$

and where the polarization fractions are expressed in terms of the cross-section ratio σ_0/σ_1. This equation is fit to the data to obtain the ratios σ_0/σ_1 and N'_{90}/N_{90}.

Measurements over a range of angles were made with a single foil. Repeated measurements at $\theta_L=90°$ were used to check for possible foil thickening or deterioration effects during a run. None were observed. Different foils ranging in thickness from 50 to 80 $\mu g/cm^2$ were used, but no significant changes in the polarization were observed over this small range of the foil thicknesses, although the thickness dependence of the ratio of the ^3P and ^1P intensities was observed.

From the fits to the reflectivity functions determined in Ref. A, it was found that

$$\sigma_0/\sigma_1=2.1\pm0.24$$

for

$$P(^1P)=0.35\pm0.05$$

and

$$\sigma_0/\sigma_1=1.5\pm0.15$$

for

$$P(^3P)=-0.11\pm0.05\,;$$

the mean value is

$$(\sigma_0/\sigma_1)_{av}=1.8\pm0.3\,.$$

From the fits to the relative intensities of the angular distributions, it was found that $\sigma_0/\sigma_1=1.79(0.1)$. The distribution at angles less than 90° was deemed less precise than the distribution at angles $\geq 90°$. This is due to larger uncertainties in the least-squares fits to the spectra at the smaller angles. Each partial distribution was separately fit, and the results combined with a weighting ratio of two to one favoring the more precise data at the larger angles, shown in Fig. 6.

Calculations of the cross sections σ_0 and σ_1 for capture to the $2P$ sublevels of sulfur from the K shell of carbon for 2-MeV/amu collisions have been carried out by Reading and Ford[15] using the "perturbative" version of their OHCE method, as well as the Oppenheimer-Brinkman-Kramers (OBK) approximation and their single-centered expansion

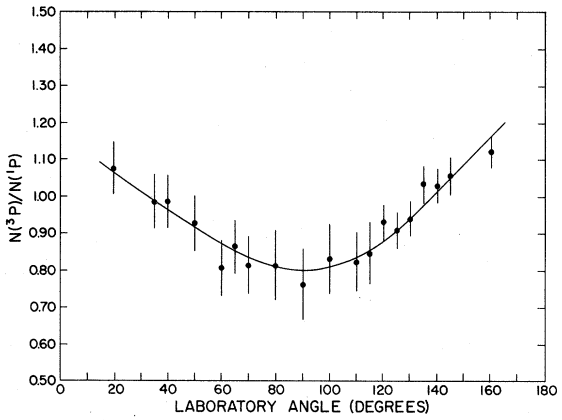

FIG. 6. Ratio of ^3P to ^1P transition intensities as a function of laboratory angle. Solid curve represents best fit to the data. Departure from symmetry about 90° is due mainly to Doppler effect.

(SCE) method. In the calculations, both the target and projectile were assumed to be hydrogenic, so the calculations specifically refer to

$$S^{16+}+C^{5+}(1s)\rightarrow S^{15+}(2P_m)+C^{6+} .$$

The absolute magnitude of the cross sections will depend somewhat on the specific atomic potentials used, primarily through the effect of screening on the orbital energies. However, the polarization fractions, which depend on cross-section ratios, are thought to be much less sensitive, and these calculations for a single-electron collision system should be a reasonable approximation to the experimental collision. Note also that the calculations were carried out for the time-reversed collision for which the electron is initially bound to the sulfur; the large set of expansion functions are centered on the sulfur ion. The experimental and theoretical results are summarized in Table I with the cross sections expressed in units of 10^{-16} cm^2. The effects of direct excitation from the $1s$ and $2s$ levels of S XVI by C^{+6} in the time-reversed collision are expected to be at the 1% level. Both the OHCE and SCE results are in agreement with the measurements, while the OBK results are not. Additionally, the OBK cross sections are about an order of magnitude larger than those calculated by the other methods. The close agreement between OHCE and SCE results for these sublevel capture cross sections is consistent with the previous calculations of total capture cross sections and supports the accuracy of the method.

The intensity ratios of the transitions from the ^3P and ^1P levels depend on the foil thickness, as noted earlier. Small variations in this thickness shift the absolute ratio, but do not significanly change the polarization fractions. It is possible that there are foil thickness and structure effects on the p-state alignment, due to the differences in the excitation mechanisms of the ^1P and ^3P levels described in Sec. I. The data analysis used here assumes that such effects are small. It was decided that a study of the target thickness dependence of the polarization fraction should be carried out using magnesium projectiles rather than sulfur projectiles, since the energy resolution is better for magnesium x rays and the structural feature lying between the ^1P and ^3P peaks is expected to contribute to a much smaller extent. This study is currently in progress.

ACKNOWLEDGMENTS

We wish to acknowledge helpful discussions with Professor A. L. Ford and Professor J. F. Reading as well as their permission to quote their unpublished calculations. This research was supported by the Department of Energy, Office of Basic Energy Sciences Division of Chemical Sciences, and the Robert A. Welch Foundation (R.L.W.), and by the National Science Foundation (D.A.C.).

TABLE I. Calculations and measurements of the cross-section ratio σ_0/σ_1 are compared. The calculations of σ_0, σ_1, and the ratio σ_0/σ_1 by three theoretical approximations are given (see text) with the derived values of the polarization fractions $P(^1P)$ and $P(^3P)$. The experimental results are the polarization fractions and the derived value of σ_0/σ_1 (Ref. A) and the ratio σ_0/σ_1 with the calculated polarization fractions (present results).

	Theory			Experiment	
	OHCE	SCE	OBK	Ref. A	Present results
σ_1	2.41×10^{-2}	2.36×10^{-2}	0.12		
σ_0	4.26×10^{-2}	4.26×10^{-2}	0.17		
σ_0/σ_1	1.76	1.80	1.42	1.8(0.3)	1.79(0.1)
$P(^1P)$	0.28	0.29	0.17	0.35(0.05)	0.28(0.05)
$P(^3P)$	−0.16	−0.17	−0.093	−0.11(0.05)	−0.16(0.03)

*Physics Department, Peking Normal University, Peking, China, on leave at Texas A&M University.
[1]H. J. Andra, Phys. Scr. 9, 257 (1974).
[2]D. A. Church and C. H. Liu, Physica (Utrecht) 67, 90 (1973).
[3]M. Hass, J. M. Brennan, H. T. King, T. K. Saylor, and R. Kalish, Phys. Rev. Lett. 38, 218 (1977).
[4]G. Goldring, Y. Niv, Y. Wolfson, and A. Zemel, Phys. Rev. Lett. 38, 221 (1977).
[5]R. L. Watson, A. Langenberg, R. A. Kenefick, C. C. Bahr, and J. R. White, Phys. Rev. A 23, 2471 (1981).
[6]R. W. Schmieder, Rev. Sci. Instrum. 45, 687 (1974).
[7]D. A. Church and C. H. Liu, Phys. Rev. A 5, 1031 (1972); P. G. Christiansen and D. F. Dalton (unpublished).
[8]C. L. Cocke, *Beam-Foil Spectroscopy,* edited by I. A. Sellin and D. J. Pegg (Plenum, New York, 1976), p. 283.
[9]J. Burgdorfer, J. Phys. B 14, 1019 (1981).
[10]D. J. Burns, R. D. Hight, and C. H. Greene, Phys. Rev. A 20, 404 (1979).
[11]J. Burgdorfer, H. Gabriel, and H. Schroder, Z. Phys. 295, 7 (1980).
[12]J. F. Reading, A. L. Ford, and R. L. Becker, J. Phys. B 14, 1995 (1981).
[13]J. F. Reading, A. L. Ford, and R. L. Becker, J. Phys. B 15, 625 (1982).
[14]A. L. Ford, J. F. Reading, and R. L. Becker (unpublished).
[15]J. F. Reading and A. L. Ford (private communications).
[16]I. C. Percival and M. J. Seaton, Philos. Trans. R. Soc. London A251, 113 (1958).
[17]U. Fano and J. Macek, Rev. Mod. Phys. 45, 553 (1973).
[18]K. A. Jamison and P. Richard, Phys. Rev. Lett. 38, 484 (1977).
[19]K. A. Jamison, P. Richard, F. Hopkins, and D. L. Matthews, Phys. Rev. A 17, 1642 (1978).
[20]K. A. Jamison, IEEE Trans. Nucl. Sci. NS-26, 1006 (1979).
[21]B. E. Warren, *X-Ray Diffraction* (Addison-Wesley, Reading, Mass., 1969).
[22]W. H. Zachariasen, *Theory of X-Ray Diffraction in Crystals* (Wiley, New York, 1945).
[23]L. D. Ellsworth, J. A. Guffey, E. Salzborn, and J. R. MacDonald, Phys. Rev. A 15, 1438 (1977).
[24]E. Horsdal Pederson, S. J. Czuchlewski, M. D. Brown, L. D. Ellsworth, and J. R. MacDonald, Phys. Rev. A 11, 1267 (1975).
[25]D. W. Wang, R. L. Watson, R. A. Kenefick, and D. A. Church, Nucl. Instrum. Methods (in press).
[26]A. Langenberg, R. L. Watson, and J. R. White, J. Phys. B 13, 4193 (1980).
[27]A. Burek, Space Sci. Instrum. 2, 53 (1976).